LATERALLY VIBRATING LITHIUM NIOBATE MEMS RESONATORS WITH 30% ELECTROMECHANICAL COUPLING COEFFICIENT

Flavius V. Pop[1,2], Abhay S. Kochhar[1], Gabriel Vidal-Álvarez[1] and Gianluca Piazza[1]
[1]Department of Electrical and Computer Engineering, Carnegie Mellon University, Pittsburgh, USA
[2]DPIA Polytechnic Department of Engineering and Architecture, University of Udine, ITALY

ABSTRACT

This paper demonstrates laterally vibrating lithium niobate (LN) microelectromechanical (MEMS) resonators operating at 500 MHz with an electromechanical coupling coefficient (k_t^2) around 30% - the highest ever attained for this class of resonators. This accomplishment is made possible by the use of direct bonding of bulk X-cut LN wafers to high resistivity silicon and a resonator electrode layout that permits harnessing the full capabilities of the film.

INTRODUCTION

The rapid growth of the Internet-of-Things (IoT) has generated significant interest for ultra-low (almost zero) power wake-up receivers. Such radios would be capable of instantaneously detecting incoming signals by being always on, hence eliminating the need for complicated scheduling algorithms and enabling much faster wake-up times. Such low power systems would ultimately eliminate the need for battery replacement and dramatically extend the lifetime of wireless sensors.

The synthesis of such wake-up receivers hinges on the ability to attain a high signal to noise ratio and high sensitivity without consuming almost any power. For this reason, passive approaches that rely on high-Q mechanical resonators to provide for voltage amplification and filtering are desirable [1]. For this purpose, we envision the realization of a very simple RF radio system such as the one shown in Fig. 1 and formed by a two chip solution including a MEMS front-end and a CMOS back-end. The mechanical resonator is used to provide for matching to the 50 Ω antenna, filtering and passive voltage amplification. A CMOS circuit is used to rectify and amplify the signal and generate a digital trigger output voltage. By resonating out the input impedance (generally capacitive) of the CMOS rectifier, we can attain filtering and voltage amplification. By ensuring that the resonator has an impedance close to 50 Ω at resonance, we can directly match to an external antenna without the need for any matching network. The resonator plays a core role in ensuring that the proposed circuit attains high sensitivity and simultaneously high rejection of interferers. It turns out that when using a simple 2-terminal mechanical resonator to implement such system the voltage amplification and out-of-band rejection are maximized when the figure of merit (FoM) of the resonator, namely the product of its quality factor, Q, and its electromechanical coupling coefficient, k_t^2, is the highest.

Rather than increasing Q, which would limit the maximum bandwidth of the communication link, we have preferred to pursue the making of resonators with a large k_t^2. The use of high k_t^2 resonators also facilitates interfacing to a 50 Ω antenna in a very small form factor.

We propose to use thin films of lithium niobate (LN) to make the resonators, since LN is a piezoelectric material that theoretically exhibits some of the highest k_t^2 when micromachined in suspended membranes. Several groups have worked on LN MEMS resonators using either ion-sliced or implanted films [2] [3], sputtered films [4] or wafer bonding and polishing [5]. Although a high k_t^2 nearing 20% has been demonstrated in specific geometries, cuts and orientations [6], no prior work has been able to fully harness the material coupling close to its theoretical limit [7]. Herein, we demonstrate, for the first time, MEMS resonators fabricated using thin films of X-Cut LN that are capable of k_t^2 around 30%, close to the maximum effectively achievable for the specific mode of vibration being excited (known as the S0 mode).

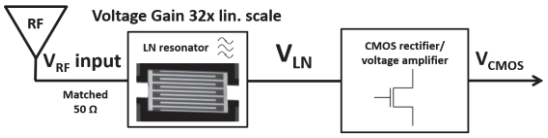

Figure 1: Envisioned 2-chip RF system comprising a LN resonator for passive amplification and filtering and a CMOS chip for signal demodulation and rectification.

In order to optimize the device Q, several parameters of the resonator geometry were varied. Experimental data show very good agreement with finite element analysis (FEA) that predicts energy loss through the anchors. Qs from 100 to 1,000 were attained with a maximum figure of merit (FoM = $k_t^2 \cdot$ Q) of 219. Such a high FoM makes these devices ideally suited for the front-end components in our envisioned receivers.

X-CUT LN RESONATOR DESIGN

The resonators are designed to vibrate in the so called symmetric Lamb wave mode of zero order (S0). The mode is excited by applying an electric field between interdigitated electrodes (IDE) made out of Al. Because of the applied electric field, strain is generated in the plane of the film through the piezoelectric effect in X-Cut LN. Since the electric field is in-line with the strain direction, the excitation method is known as in-line excitation (see Fig. 2). The device is placed at a specific angle (30º) with respect to the Y axis so as to maximize the resonator k_t^2 [7]. The device resonant frequency, f_s, is set by the pitch of the IDE according to the following equation:

$$f_s = \frac{1}{\lambda}\sqrt{\frac{E_p}{\rho}} \quad (1)$$

where $\lambda = 2 \cdot$pitch is the resonant acoustic wavelength, E_p is the equivalent Young's modulus of the LN along the direction of vibration and ρ is its mass density. In order to fully harness the k_t^2 of the material, the electrodes at the two free edges of the resonator (see Fig. 3) were designed

to behave as λ/4 reflectors and maximize the efficacy with which the desired S0 mode is excited [8]. Similarly, the electrode coverage was selected to be 1/3 of the IDE pitch as it results in maximum electromechanical coupling [9].

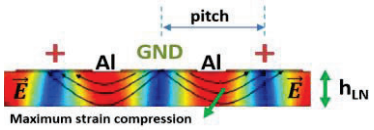

Figure 2: S0 mode excitation in a LN thin film through the use of interdigitated Al electrodes. Some characteristic device parameters are labeled in the figure.

In Fig. 3 we present a top view of the geometry of a LN resonator. The device is suspended through two anchors, which are also used to route the two electrical terminals, respectively through Port 1 (RF input) and Port 2 (RF output). Important geometrical parameters such as the anchor size (*Wa* and *La*), the width of the bus (*Wb*) and the width of the gap (*Wg*) between the bus and the end of the IDE were varied to study their impact on the resonator damping.

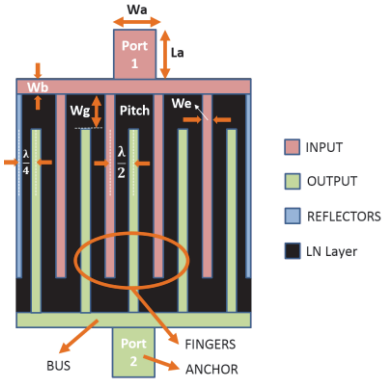

Figure 3: Designed geometry of the LN resonator. Parameters are described in Table 1.

COMSOL Finite Element Analysis (FEA) was used to simulate the impact of the resonator geometry (Fig. 4) on *Q* by using Perfectly Matched Layers (PMLs), hence mimicking the effect of anchor losses [10] [11]. The action of the PMLs is to absorb all the outgoing waves from the anchors as it would happen with a real device.

An important aspect of the FEA simulation is the meshing of the geometry as this can impact the accuracy of the modeling results. For this reason, we used tetrahedral elements with different dimensions, going from λ for the external PML to λ/10 for smaller elements forming the bus and the electrodes (Fig. 5).

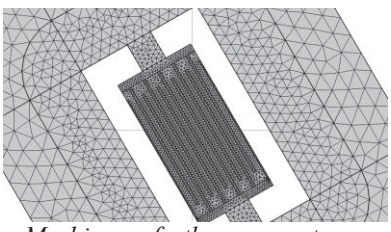

Figure 5: Meshing of the resonator geometry in COMSOL. Here we can notice different mesh sizes going from very coarse steps of λ for the PML layer to very fine steps of λ/10 for the IDE.

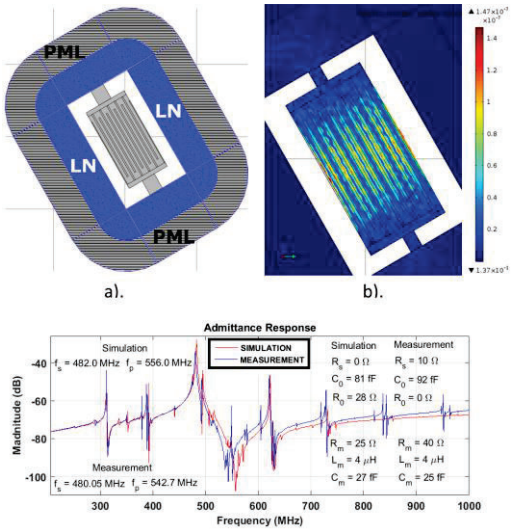

Figure 4: (a) Resonator geometry used in COMSOL FEA. (b) Resonator's displacement at resonance highlighting the mode shape (S0) of the laterally vibrating resonator. (c) Comparison of the admittance magnitude over frequency between COMSOL simulation and experimental results. We can notice a down-shift of the anti-resonance due to parasitic capacitance . This is directly responsible for a slight k_t^2 degradation.

FABRICATION METHOD

The accomplishments reported in this paper were made possible by the use of bulk quality X-cut LN films directly bonded to a high resistivity silicon wafer. 1 µm thin film of X-cut LN is prepared by surface activation bonding of a 4" LN wafer to Si and by polishing the LN to the desired thickness. The fabrication of the device is shown in Fig. 3. It is based on standard LN etching and metal lift-off steps. Resonators of various dimensions (electrodes numbers, different anchors and bus, LN plate width and length etc.) were laid out (Table 1). Particular attention was placed in the definition of the electrodes at the free end of the resonator (W_g), which are critical in ensuring maximum coupling into the desired mode of vibration [12].

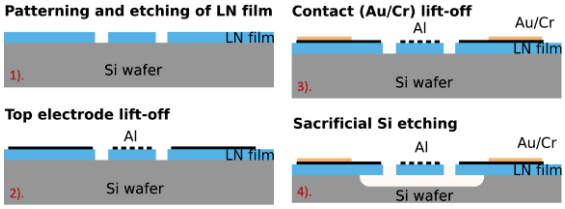

Figure 6: Fabrication process flow. 1) In order to ensure good film uniformity across a 4" wafer, the Si wafer had to be flatten to have a total thickness variation < 1 µm. PECVD deposited SiO_2 is used as a mask for patterning the LN film. Cr is sputtered on SiO_2 and later dry etched, acting as a metal mask for etching SiO_2. For etching of Cr and LN, Cl_2-based ICP RIE is utilized. For SiO_2 etching, fluorine-based parallel plate RIE is used. After etching of LN, the SiO_2 mask is removed in a wet buffered HF solution. 2) Later, Al (top electrode) and 3) Au/Cr (contact) patterning is completed using lift-off. 4) Finally, devices are released by sacrificially etching silicon using XeF_2 vapor phase etching.

As a result of the fabrication, in Fig. 7 we can see an SEM image of a device with 9 electrodes and 2 reflectors. Diffrent views are showed focusing on various elements of the resonator and on its sidewall.

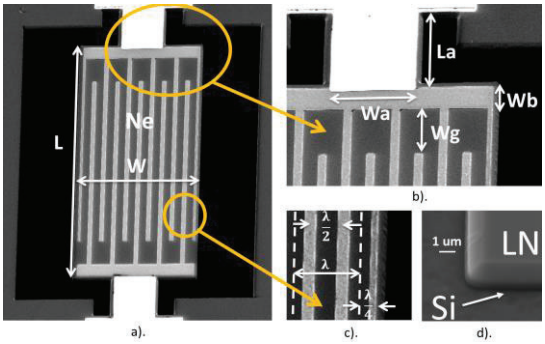

Figure 7: SEM images of LN LVR and its geometrical parameters (see Table 1). (a) Top view of the resonator. (b) Zoom on anchor, bus and edge reflector. (c) Zoom on electrode pitch and reflecting edge (reflectors). (d) Cross-section view showing the LN sidewall.

Table 1: Main geometrical resonator parameters and actual values explored in this work.

Parameter	Description	Values
λ	Acoustic wavelength	12 [μm]
pitch	Electrode center to center separation	6 [μm] (λ/2)
We	Electrode width	2 [μm] (λ/6)
Ne	Electrodes number	10, 20, 30, 40, 60
L	LN plate length	60, 90, 120 [μm]
W	LN plate width	60,120,180,240, 360 [μm]
La	Anchor length	21,21.5,22.5[μm]
Wa	Anchor width	19.5, 21 [μm]
Wb	Bus width	3, 4.5, 6, 9 [μm]
Wg	Gap between the electrode's free end and the bus	4.5, 6, 9, 12 [μm]

EXPERIMENTAL RESULTS

The fabricated devices were wafer probed in laboratory conditions (without any temperature or humidity control). Each device was tested in a 2-port configuration by connecting its two terminals (see Fig. 3) to two ports of a vector network analyzer. The 2-port S-parameters were converted into equivalent Y-parameters and used to extract the device performance. Specifically, Y_{21} (equal to Y_{12} for these devices) was fitted to the equivalent modified Butterworth Van Dyke (MBVD) circuit model [11to13], shown in Fig. 8. Note that the use of Y_{21} permits to directly extract the intrinsic resonator parameters without the need for de-embedding.

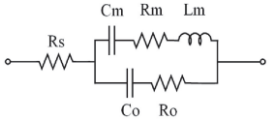

Figure 8: MBVD equivalent electrical model of the LN resonators of this work. This model was fitted to the Y_{21} response of the resonator.

The motional parameters of the circuit components can be approximated to the following:

$$C_m = \frac{8}{\pi^2} C_0 k_t^2 \tag{2}$$

$$R_m = \frac{\pi^2}{8} \frac{1}{\omega_s C_0} \frac{1}{k_t^2 Q} \tag{3}$$

$$L_m = \frac{\pi^2}{8} \frac{1}{\omega_s^2 C_0} \frac{1}{k_t^2} \tag{4}$$

where ω_s is the resonance frequency and C_0 is the static capacitance of the resonator. These parameters were directly extracted from the Y_{21} response and not derived based on the measured values of k_t^2 and Q. C_0 and R_0 are extracted from the out-of-resonance response, respectively from the imaginary and real part of the device's admittance. R_s instead is measured directly on the wafer and represents the series resistance of the routings to the resonator.

k_t^2 and Q are extracted using the expression in Equations (5) and (6):

$$Q = \frac{f_s}{\Delta f_{3dB}} \tag{5}$$

$$k_t^2 = \frac{\pi^2}{8} \frac{f_p^2 - f_s^2}{f_p^2} \tag{6}$$

where f_s is the resonance frequency and f_p is the anti-resonance (parallel) frequency of the resonator. It is important to note that Eq. (6) that was used to extract the resonator k_t^2 is an approximation of the exact formula shown in [14].

Using the aformentioned equations, the best device exhibited a k_t^2 of 30% and Q of 737, resulting in a FoM of 219. Its response (overlapped with fitted parameters) is shown in Fig. 9.

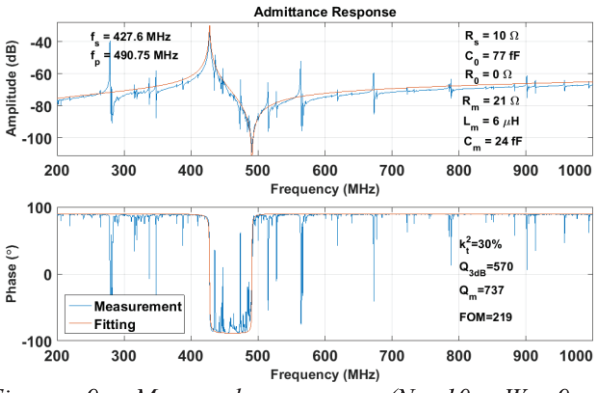

Figure 9: Measured response (Ne=10, Wg=9μm, Wb=6μm, La=22.5μm, Wa=19.5μm, W=60μm, L=120μm) of the X-Cut LN resonator with the highest recorded FoM. The response (blue curve) was fitted (red curve) to the equivalent electrical model shown in [13].

A group of devices with the same plate size (W=60μm, L=120μm] but different bus width and different gap between the bus and the free end of the electrodes were also tested and the Qs were monitored against FEA predictions (Fig. 10). Based on these experimental data, we conclude that the Q of these devices is currently limited by anchor losses. In

particular, the use of Au on the anchor, the width of the bus and the separation between the electrode and the free edge of the resonator play a key role in setting Q.

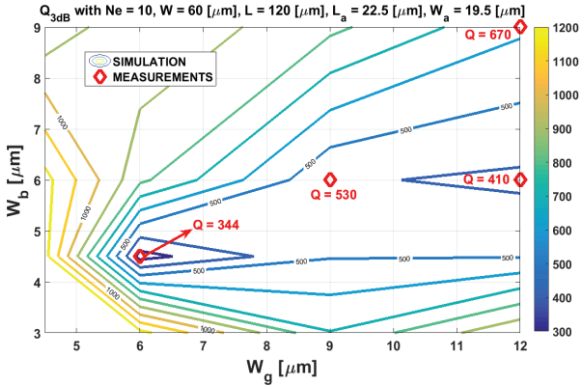

Figure 10: Contour plot of device's Q as a function of anchor losses according to FEA. Experimental data are overlapped to showcase close matching to theoretical predictions.

CONCLUSION

We have demonstrated X-Cut LN resonators exhibiting a k_t^2 that is effectively approaching the maximum predictable by simulations [7]. In future fabrications, we plan to layout devices with different orientations and confirm experimentally the k_t^2 model predicted by simulations [7].

We also plan to improve the resonator FoM, which is currently set at a maximum of 219, by increasing the *Q* through further investigation of the impact of the resonator geometry on damping.

ACKNOWLEDGEMENTS

The material is based upon work supported by the Defense Advanced Research Projects Agency (DARPA) under Contract No. HR0011-15-C-0137.

REFERENCES

[1] S. Gong and G. Piazza, "Monolithic Multi-Frequency Wideband RF Filters Using Two-Port Laterally Vibrating Lithium Niobate MEMS Resonators," in *Journal of Microelectromechanical Systems*, vol. 23, no. 5, pp. 1188-1197, Oct. 2014.

[2] R. Wang, S. A. Bhave, S. Zhgoon and K. Bhattacharjee, "Multi-frequency LiNbo3 Lamb wave resonators with < 3 Ω impedance," *2016 IEEE 29th International Conference on Micro Electro Mechanical Systems (MEMS)*, Shanghai, pp. 679-682, 2016.

[3] R. H. Olsson III, K. Hattar, S. J. Homeijer, M. Wiwi, M. Eichenfield, D. W. Branch, M. S. Baker, J. Nguyen, B. Clark, T. Bauer, T. A. Friedmann, "A high electromechanical coupling coefficient SH0 Lamb wave lithium niobate micromechanical resonator and a method for fabrication", *Sensors and Actuators A: Physical*, Vol. 209, pp. 183-190, March 2014.

[4] M. Kadota, T. Ogami, K. Yamamoto, H. Tochishita and Y. Negoro, "High-frequency lamb wave device composed of MEMS structure using $LiNbO_3$ thin film and air gap," in *IEEE Transactions on Ultrasonics, Ferroelectrics, and Frequency Control*, vol. 57, no. 11, pp. 2564-2571, November 2010.

[5] R. Wang, S. A. Bhave and K. Bhattacharjee, "Design and Fabrication of S_0 Lamb-Wave Thin-Film Lithium Niobate Micromechanical Resonators," in *Journal of Microelectromechanical Systems*, vol. 24, no. 2, pp. 300-308, April 2015.

[6] J. Blanckenstein, J. Klaue and H. Karl, "A Survey of Low-Power Transceivers and Their Applications," in *IEEE Circuits and Systems Magazine*, vol. 15, no. 3, pp. 6-17, 2015.

[7] I. E. Kuznetsova, B. D. Zaitsev, S. G. Joshi and I. A. Borodina, "Investigation of acoustic waves in thin plates of lithium niobate and lithium tantalate," in *IEEE Transactions on Ultrasonics, Ferroelectrics, and Frequency Control*, vol. 48, no. 1, pp. 322-328, Jan. 2001.

[8] S. Gong and G. Piazza, "Weighted electrode configuration for electromechanical coupling enhancement in a new class of micromachined Lithium Niobate laterally vibrating resonators," *2012 International Electron Devices Meeting*, San Francisco, CA, 2012, pp. 15.6.1-15.6.4.

[9] L. Shi and G. Piazza, "Active reflectors for high performance lithium niobate on silicon dioxide resonators," *2015 28th IEEE International Conference on Micro Electro Mechanical Systems (MEMS)*, Estoril, 2015, pp. 992-995.

[10] J. Segovia-Fernandez, C. Xu, C. Cassella and G. Piazza, "An alternative technique to Perfectly Matched Layers to model anchor losses in MEMS resonators with undercut suspensions," *2015 Transducers - 2015 18th International Conference on Solid-State Sensors, Actuators and Microsystems (TRANSDUCERS)*, Anchorage, AK, pp. 985-988, 2015.

[11] L. Shi and G. Piazza, "Investigations on quality factor of high frequency laterally vibrating LN on SiO2 microresonators," *2014 IEEE International Ultrasonics Symposium*, Chicago, IL, pp. 578-581, 2014.

[12] S. Gong and G. Piazza, "Figure-of-Merit Enhancement for Laterally Vibrating Lithium Niobate MEMS Resonators," in *IEEE Transactions on Electron Devices*, vol. 60, no. 11, pp. 3888-3894, Nov. 2013.

[13] J. D. Larson, P. D. Bradley, S. Wartenberg and R. C. Ruby, "Modified Butterworth-Van Dyke circuit for FBAR resonators and automated measurement system," *2000 IEEE Ultrasonics Symposium. Proceedings. An International Symposium (Cat. No.00CH37121)*, San Juan, vol.1, pp. 863-868, 2000.

[14] "IEEE Standard on Piezoelectricity," *ANSI/IEEE Std 176-1987* , 1988.

CONTACT

*F.V. Pop, flaviusvasile.pop@gmail.com, fpop@andrew.cmu.edu

*G. Piazza, tel: +1-412-268-7762; piazza@ece.cmu.edu